

Peculiarities of Microwave Emission from Active Regions Generating Intense Solar Flares

V. M. Bogod* and S. Kh. Tokhchukova

*Special Astrophysical Observatory, Russian Academy of Sciences,
Nizhnii Arkhyz, Stavropolskii Krai, 357147 Russia*

Received August 28, 2002

Abstract—RATAN-600 multiwavelength observations of the Sun reveal sharp spectral inhomogeneities in the polarized radiation from active regions that produce intense flares. These events occur in a wide range of radio fluxes (0.05–10 s.f.u.) in a relatively narrow wavelength range (2–5 cm). They are detected on times scales from several hours to several days before and during an intense flare. We analyze the detected events and their relationship to the preliminary phase of intense flares. Significant statistical material was obtained in 2001. The new flare-plasma properties can be used to test existing solar-flare models and to develop new criteria of flaring activity. © 2003 MAIK “Nauka/Interperiodica”.

Key words: *Sun, solar radio emission, polarization, solar flares.*

INTRODUCTION

Studying the preflare plasma is important both in understanding the processes that lead to a flare and in developing criteria for predicting the flaring activity and, in particular, the proton activity. Such studies are being carried out in a wide frequency range, including ultraviolet, X-ray, optical, and radio satellite observations. Since flares most often originate in the upper chromosphere and the lower corona and subsequently extend to higher levels (into the X-ray corona) and to lower-lying levels (into the optical photosphere), it should be assumed that the main preflare-plasma properties must clearly show up precisely in the radio frequency range.

Varied and long-term studies using various radio instruments revealed a number of preflare-plasma properties. The criterion of Tanaka and Enome (1975), which is used to compare polarization measurements at two wavelengths (3 and 8 cm), is widely known. The reliability of this criterion was high (~70%) in solar cycle 20 and decreased sharply in the next cycle.

We know the flare precursors—small increases in the total solar flux 20–40 min before a flare (Pustil'nik 1983), increases in the total radio flux fluctuation 20–40 min before a flare (Kobrin *et al.* 1978), and decreases in the radio flux before a flare (Covington 1973). Recently, Kundu *et al.* (2001) have reported radio fluctuations several minutes before a flare, which correlated with X-ray fluctuations.

High-spatial-resolution observations revealed a prolonged microwave darkening of an active region (AR) before a flare (Bogod *et al.* 1999), the emergence of peculiar sources (Lang *et al.* 1993) and sources above the neutral magnetic field line (Kundu *et al.* 1985), and the existence of active longitudes (Maksimov *et al.* 1988).

Since the sensitivity of radio waves to variations in chromospheric magnetic fields is high (Bogod *et al.* 1993; Nindos *et al.* 2000), various methods of their measurements were developed (Gelfreikh 1994; Ryabov *et al.* 1999) based on detailed spectral and polarization analyses in a wide wavelength range. Although there are various radio telescopes with a high spatial resolution in the world (from interferometric radioheliographs to reflective antennae), the spectrum is analyzed in detail only with two telescope: RATAN-600 (Korol'kov and Parijskij 1979) and OVRO (Hurford *et al.* 1984), which completely cover the frequency range 1–18 GHz. The latter analyzes this frequency range sequentially, passing from one frequency to another, and has narrow pass bands, which significantly reduces the polarization measurement sensitivity. RATAN-600 has broader pass bands in the frequency channels, performs a simultaneous analysis with a frequency resolution of about 5%, and has a large effective area. However, this instrument has a one-dimensional beam, which reduces its efficiency when studying weak sources because of the influence of spurious sources (confusion effect). However, when studying bright ARs, this effect is negligible. We have been using the mode of multiple azimuthal observations (with

*E-mail: vbog@gao.spb

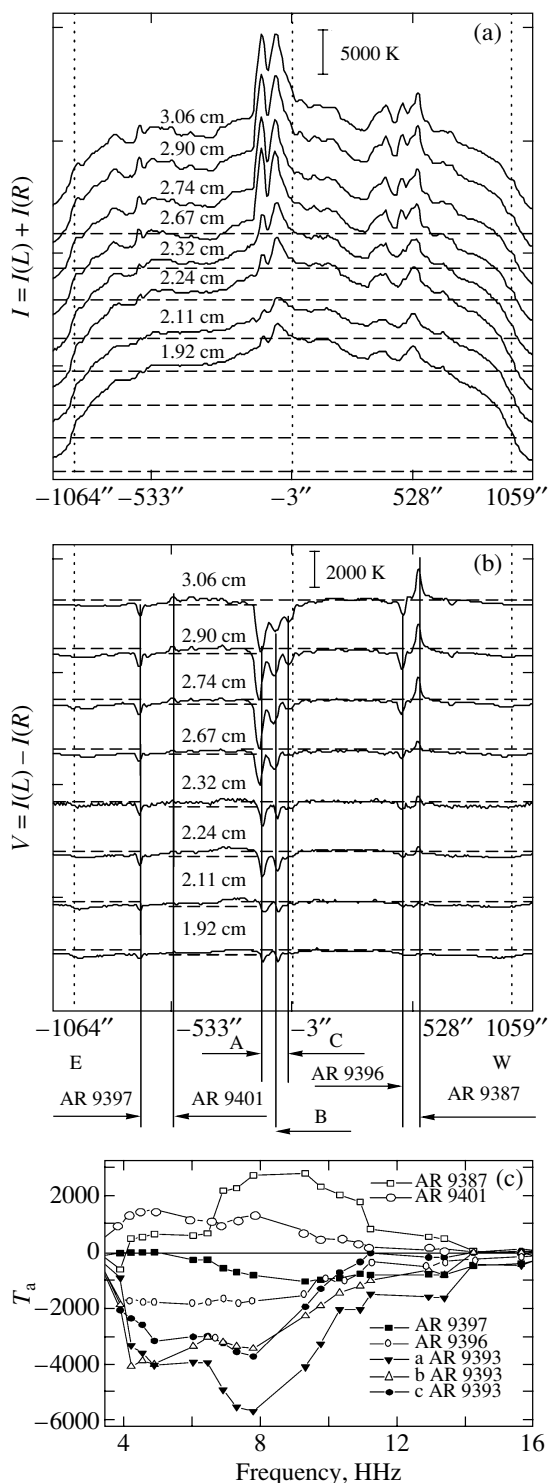


Fig. 1. The solar-disk scans for March 27, 2001, obtained with the RATAN-600 one-dimensional beam at several close centimeter wavelengths: (a) the intensity scans vertically displaced from each other for the convenience of comparison; (b) the vertically displaced circular polarization scans (in this figure and below, the signs of the left- and right-hand circular polarizations are positive and negative, respectively); (c) the maximum-amplitude spectra of polarized radio sources for the ARs shown in the upper Figs. 1a and 1b

a sampling interval of 4–8 min/scan) on RATAN-600 since 2000. This mode significantly improved the reliability of spectral measurements of the polarized radiation from ARs and allowed a number of events directly related to flaring activity to be detected in a wide time interval.

Observations reveal ARs on the Sun that differ in stability. Stable ARs produce virtually no flares over the entire period of their presence on the disk. These regions have a stable magnetic-field structure at the photospheric level and monotonic radio intensity and polarization spectra in the microwave range with a peak near 5–6 cm (Bogod *et al.* 1999; Gary *et al.* 1997) (see also Fig. 1). The behavior of these spectra is determined by the combined action of thermal mechanisms [cyclotron bremsstrahlung at the first three or four gyrofrequency harmonics (Zheleznyakov 1977; Akhmedov *et al.* 1982)]. The cyclotron radiation from an AR has a circular polarization that corresponds to an excess of the extraordinary-wave radiation and the polarization sign is determined by the magnetic-field polarity of the dominant sunspot.

Of particular interest are flare-productive active regions (FPARs), which are distinguished by flux variability and high flaring activity. Our study of FPARs indicates that microwave spectral-polarization observations are highly informative; they appear to directly detect plasma at the sites of primary energy release before a flare. Several new manifestations were found in the radio polarization spectrum of FPARs on time scales from several hours to several days before and during a flare. We also show that these new effects are associated with the generation of intense flares and that they can be used to test existing solar-flare models [see Syrovatskii *et al.* (1983) and the reviews of Altyntsev *et al.* (1982) and Shibata (1998)] and to develop more efficient prediction criteria than the existing ones.

OBSERVATIONS

For our analysis, we used the regular spectral-polarization observations of the Sun carried out in 2001 with the RATAN-600 radio telescope. This telescope has the parameters that are currently most suitable for studying the flare plasma at early stages of FPAR activity. The most important quality of this instrument was the combination of an instantaneous frequency spectrum from 16 to 1 GHz taken with a panoramic spectrum analyzer (PSA) (Bogod *et al.* 1999) (in this work, we used the frequency range 4–16 GHz) with a frequency resolution of about 5–7%, a high sensitivity to variations in circular polarization (about 0.05%), and a high flux sensitivity reaching 0.001 s.f.u. (1 s.f.u. = 10^{-22} W m $^{-2}$ Hz $^{-1}$). Such a

high sensitivity was achieved due to a broad band of received frequencies (200–600 MHz), a simultaneous analysis of the spectrum, and a large collecting surface area ($\sim 400\text{--}600\text{ m}^2$). The RATAN-600 radio telescope has a moderate spatial resolution in the horizontal plane ($<15''$ at a wavelength of 2 cm) and a low resolution in the vertical plane ($\sim 15'$ at 2 cm). The beam size is proportional to the wavelength. Our observations were performed regularly both in single-scanning mode (three to five observations per day) and in multiple azimuthal scanning mode (23–25 scans per day at 8-min intervals for 4 h). Such frequently repeated scans with a narrow beam for 4 h allow the radiation from individual components of the AR structure (local sources above sunspots, interspot sources, flocculi, and others) to be clearly separated.

For our analysis, we used the observational data obtained in the regular RATAN-600 observations from January 4 through October 28, 2001, except for small technical interruptions from April 16 until April 24 and from August 15 until August 25. Nevertheless, almost all of the FPARs present on the disk for ten months were recorded in their spectral observations in intensity (the Stokes parameter $I = I(L) + I(R)$) and polarization ($V = I(L) - I(R)$). In addition, we carried out multi-azimuthal observations, which allowed the dynamic properties of FPARs to be studied at microwaves.

Figure 1a shows one-dimensional RATAN-600 scans of the Sun. For the convenience of comparison, the scans at different wavelengths were vertically displaced from one another. The observations were reduced with the Workscan code (Garaimov 1997), which is freely available at <http://www.sao.ru/~sun>. Observations of the Toyokawa flux service at frequencies of 1.0, 2.0, 3.75, and 9.4 GHz, which are published on the Internet at <ftp://solar.nro.nao.ac.jp/pub/norp/data/daily/>, were used to calibrate and reference the scans at different wavelengths. The flux at intermediate PSA frequencies is determined by a cubic interpolation and is used to calibrate the Stokes parameter $I = I(L) + I(R)$. The Stokes parameter $V = I(L) - I(R)$ is calibrated proportionally to the original signal.

Short-Wavelength Polarization Inversion in FPARs

Figures 1a and 1b show one of the multiwavelength observations performed on March 27 at 8^h50^m UT. On this day, all of the ARs detected on the solar disk were stable and their intensity (Fig. 1a) and circular polarization (Fig. 1b) spectra monotonically rose with wavelength. This behavior is typical of the radiation from stable cyclotron radio

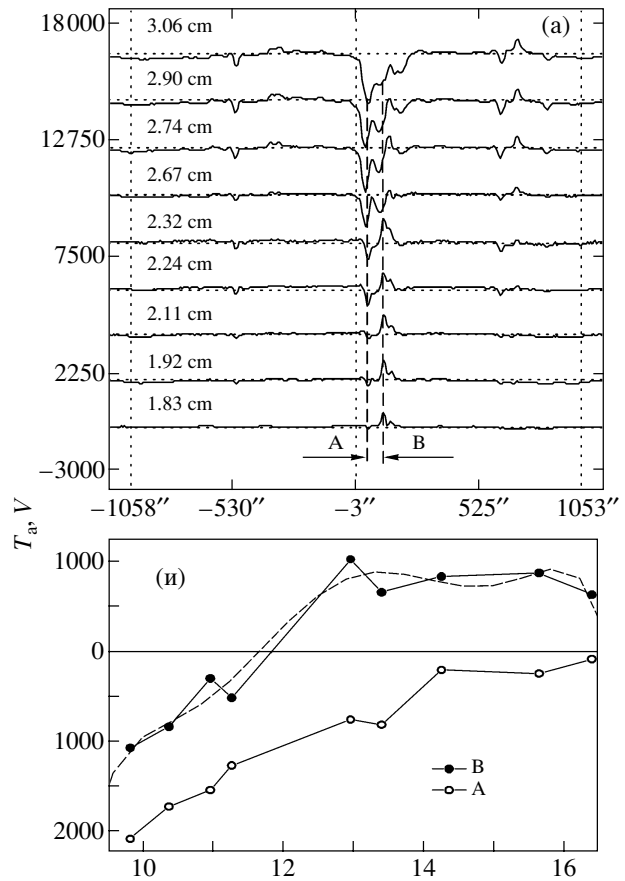


Fig. 2. (a) Circular polarization scans for the Sun at short centimeter wavelengths on March 28, 2001, 8^h46^m UT. Source A of left-hand circular polarization at wavelengths from 1.83 to 2.32 cm exhibits a rise in the western part of AR 9393, which caused a short-wavelength polarization inversion. (b) The spectra of the eastern (B) and western (A) sources in AR 9393. Source B exhibits a sign inversion at a frequency close to 12 GHz. The dotted line represents a power-law polynomial fit. Source A shows a monotonic rise in right-hand circular polarization with wavelength.

sources. The polarization spectra for some of the ARs present on the disk on this day are shown in Fig. 1c. They all exhibit a rise with wavelength at frequencies above 15 GHz and a broad peak in the frequency range 6–8 GHz. The AR NOAA 9393 (see Figs. 1a and 1b) was near the disk center. It had a complex structure that consisted of three sources of right-hand circular polarization (a, b, and c) and was flare-active, although the radiation from this region was stable during March 27, 2001. Subsequently, this AR was activated sharply, which gave rise to spectral inhomogeneities in the polarized radiation (see below).

Preflare processes began in AR 9393 on the next day. They were accompanied by a circular polarization inversion at short wavelengths (1.83–2.32 cm) in its

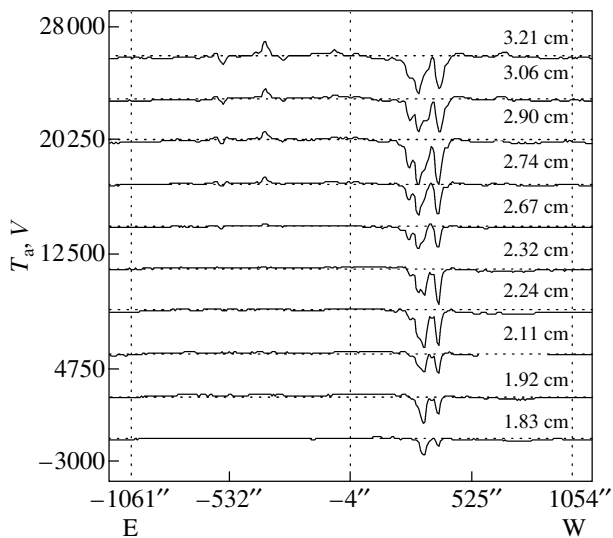


Fig. 3. Polarization scans (in antenna temperatures) for March 30, 2001, 10^h14^m UT. AR 9393 lies in the western part of the solar disk and again has a stable spectrum.

western part (see Fig. 2a). This figure shows, on a large scale, the multiwavelength one-dimensional scan for the Sun in polarized radiation obtained on March 27, 2001, at 8^h46^m UT.

On this day, AR 9393 was located near the disk center and significant changes occurred in its structure. The two main sources, B in the western part of the AR and A in its eastern part, are marked in Fig. 2a. A polarization inversion was detected in the radiation from source B at wavelengths from 1.83 to 2.32 cm, whereas the polarization pattern and sign of source A did not change (see also Figs. 1b and 2b). This short-wavelength circular polarization inversion (which we called an A1 effect) persisted until the onset of the impulsive phase of an intense X1.7 flare at 10^h15^m on March 29, 2001.

We believe that the circular polarization inversion points to a rise in the new magnetic flux whose polarity is opposite to the polarity of the overlying magnetic field with a strength of about 1400–2000 G under the assumption of cyclotron radiation at the third gyrofrequency harmonic in accordance with the formula $B[G_S] = 3570/\lambda[\text{cm}]$. In this case, the polarization sign is determined by the radiation of an extraordinary wave and the magnetic-field polarity. In general, the short-wavelength polarization inversion first appears at the shortest wavelength of 1.74 cm and then gradually displaces with time toward longer wavelengths, 3–4 cm. This type of polarization inversion should be distinguished from the well-known passage of the cyclotron radiation from a spotted radio source through a region of quasi-transverse magnetic fields (Cohen 1960; Zheleznyakov 1964; Ryabov *et al.* 1999).

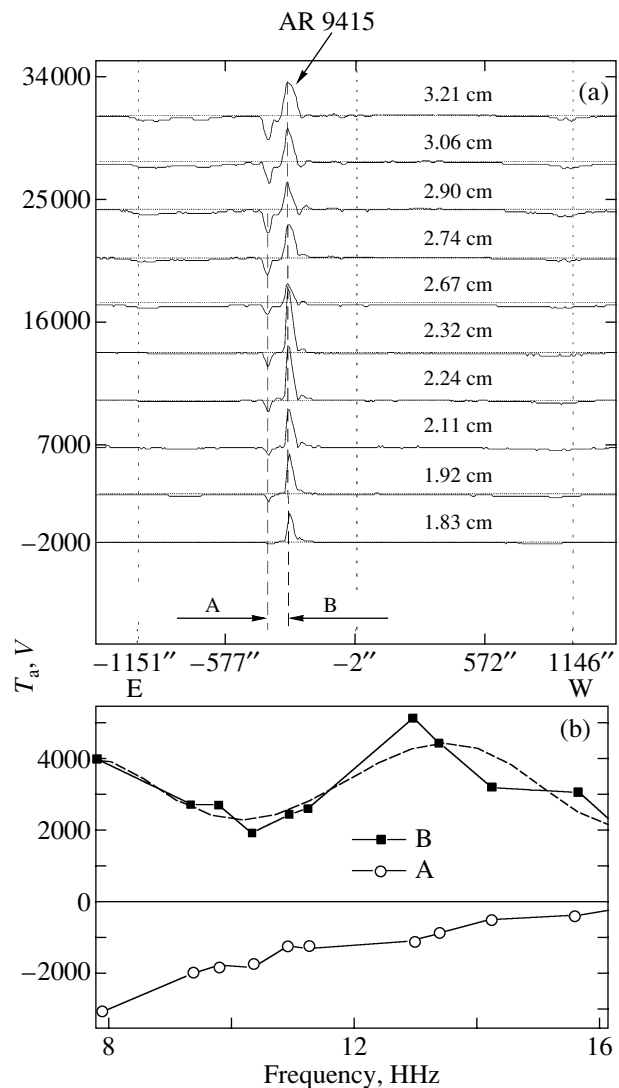


Fig. 4. (a) Polarization scans for the Sun (in antenna temperatures) on April 8, 2001, 9^h15^m UT. AR 9415 lies in the eastern part of the solar disk and has a bipolar polarization pattern in the form of sources A and B. Source A exhibits a rise in intensity at short wavelengths, while source B shows no such dependence. (b) The spectra of the western (A) and eastern (B) sources in AR 9415. Source B shows a monotonic rise in left-hand circular polarization; source A of left-hand polarization exhibits a rise of the spectrum at short wavelengths. The dotted line represents a power-law polynomial fit.

The inversion in quasi-transverse magnetic fields is known from observations to commonly begin at long wavelengths (in the range 8–9 cm) in stable ARs near the limb and displaces with time toward shorter wavelengths. On the next day, in the observations of March 30, 2001, a stable structure (see Fig. 3) similar to the structure (see Fig. 1) observed on March 27, 2001, was restored in AR 9393.

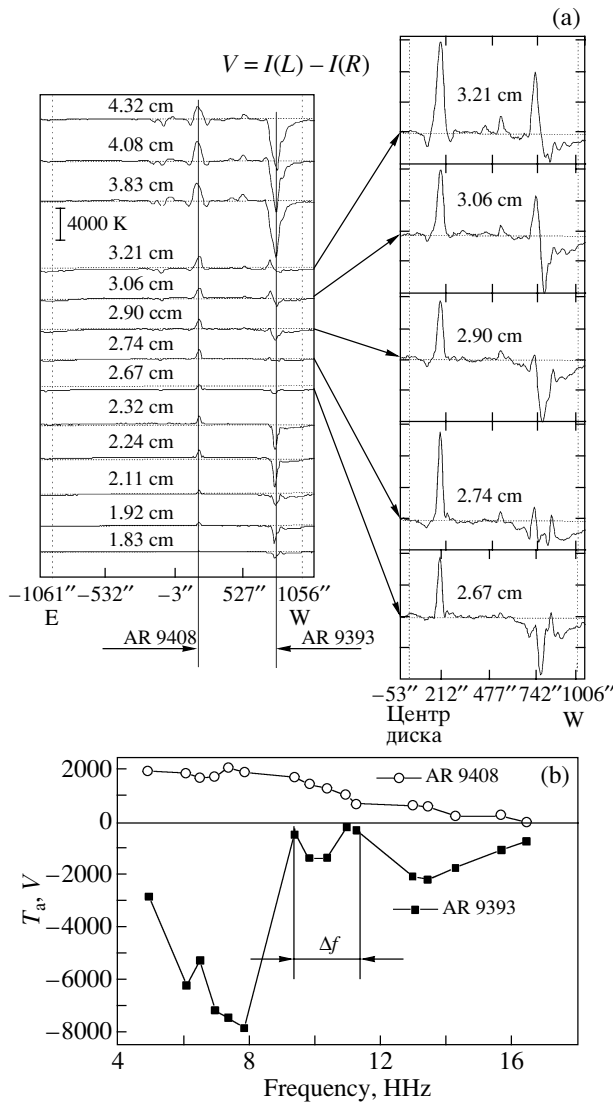


Fig. 5. (a) Polarization scans for the Sun on April 1, 2001, 9^h17^m UT. AR 9393 lies in the western part of the solar disk and has a simple polarization pattern at short (2.32 cm or shorter) and long (3.83 cm or longer) wavelengths. The scans in the wavelength range from 2.67 to 3.21 cm are shown on the right on a large scale. This range exhibits a complex pattern of mode coupling with the appearance of narrow pointlike sources, with sharp spectral slopes, polarization inversions, and a low degree of polarization. (b) The circular polarization spectra for the stable AR 9408 and FPAR 9393. Here, Δf is the width of the frequency band in which abrupt variations occur at a low level of the polarized signal.

Short-Wavelength Polarization Brightening in FPARs

Another commonly encountered effect is a brightening at short centimeter wavelengths. In Fig. 4a, this effect is illustrated for AR 9415: an increase in the circularly polarized flux is observed at short wavelengths for the western source of this group.

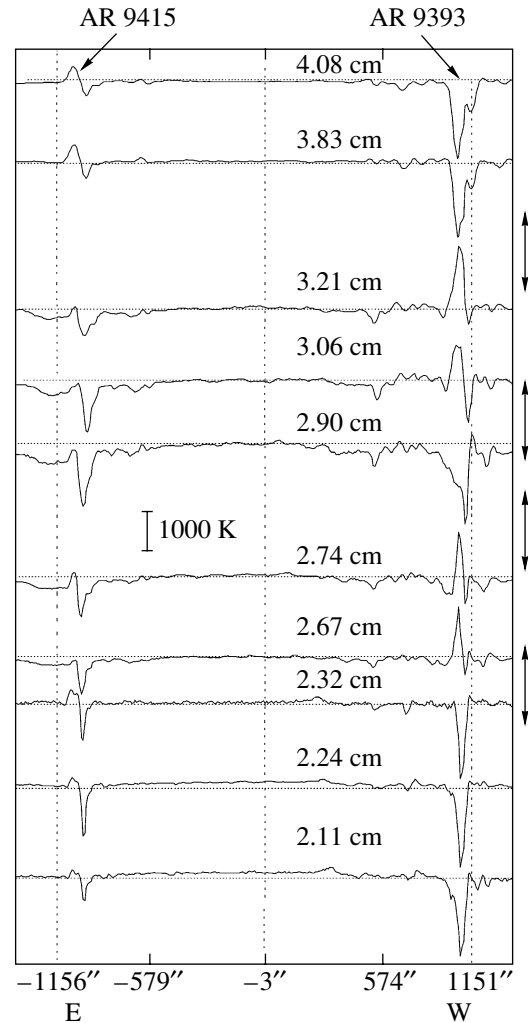


Fig. 6. Multiwavelength scans in the polarization channels at 9^h08^m UT. The arrows on the right indicate the locations of the frequency polarization inversions occurred in AR 9393 before an M8.4 flare.

We call this case an A2 effect. We believe that this effect is related to the rise of a new magnetic flux whose polarity matches the polarity of the overlying magnetic field. The spectrum exhibits a rise toward shorter wavelengths (see Fig. 4b).

The A1 and A2 effects persist from several hours to several days. The maximum frequency band in which the two effects occur is broad and reaches one octave (from 1.7 to 3.5 cm). The polarized fluxes typically lie within the range 0.05–0.5 s.f.u.; the A effects are commonly observed in FPARs (in 60% of the cases).

A Frequency-Limited Mode Coupling Region in the Radio Polarization Spectrum

The next manifestation of FPARs called a B effect is usually recorded in well-developed ARs with

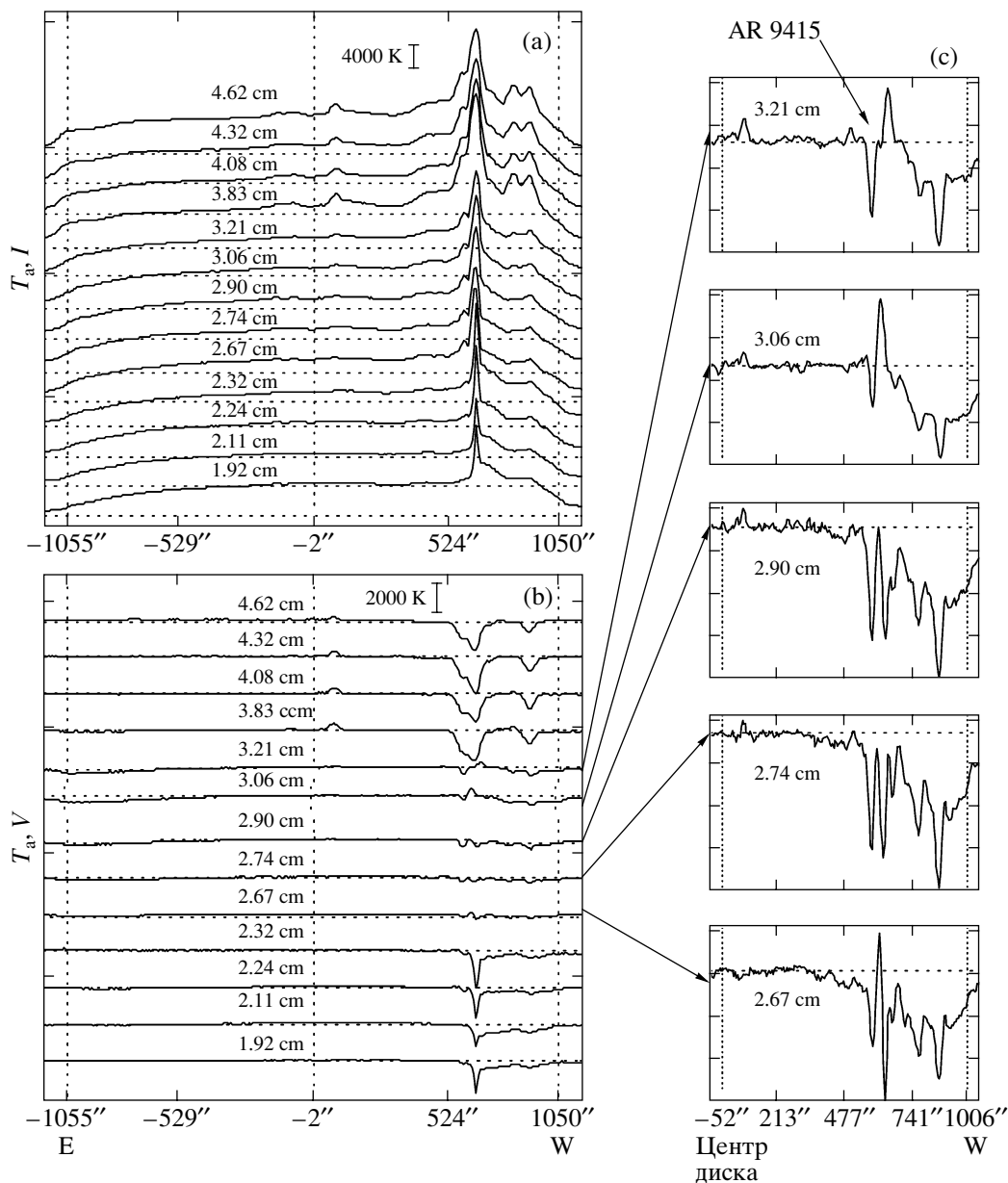


Fig. 7. The observations of April 14, 2001. The FPAR 9415 lies in the western part of the solar disk. (a) Intensity scans for the Sun; (b) circular polarization scans; and (c) scans for the western part of the solar disk on a large scale in the wavelength range 2.67–3.21 cm. The polarization pattern of AR 9415 in this range differs sharply from its pattern at short and long wavelengths, forming the so-called frequency mode coupling region.

prolonged flaring activity. This effect often results from the development of the A1 effect with time. In this case, the polarization inversion displaces toward longer wavelengths, while at short wavelengths, polarized radiation with the original polarization sign appears. The region of the B effect is characterized by a decrease of the polarized flux in a narrow frequency band (20–30%) in the wavelength range 2–5 cm. Accordingly, the degree of polarization decreases from 10–15% outside the band to fractions of a percent inside the band. In addition, narrow pointlike source

with sharp spectral slopes and multiple polarization inversions in frequency appear in this region. Figure 5 illustrates the formation of the B effect at wavelengths 2.67–3.21 cm for AR 9393. We see the appearance of new (pointlike) sources with multiple polarization inversions within a limited band at neighboring wavelengths. This band often displaces toward longer wavelengths immediately before the flare itself. In this case, an intense X20 flare occurred on April 2 at 3^h25^m UT.

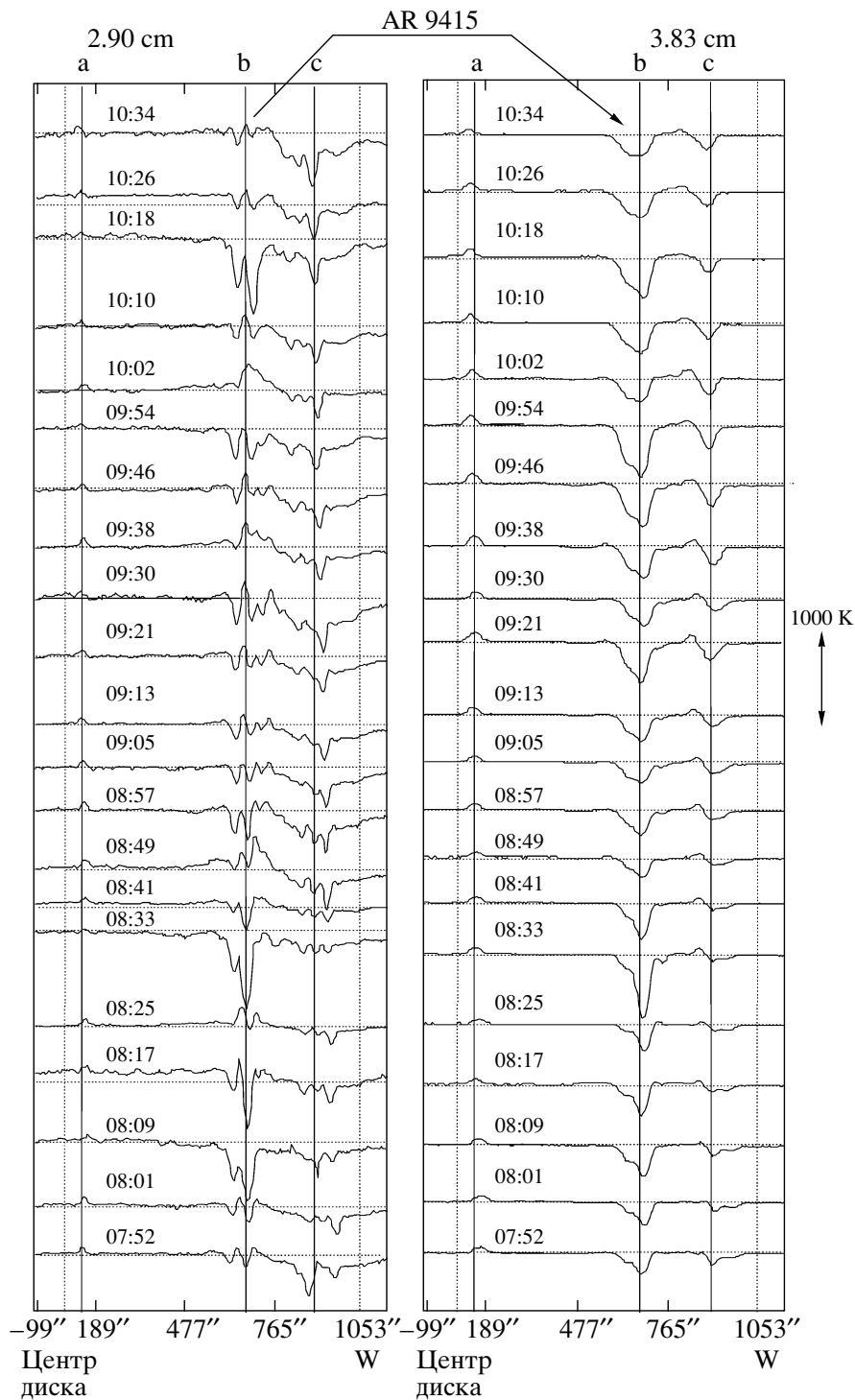


Fig. 8. An example of the dynamic polarization behavior for the FPAR 9415 at two wavelengths inside and outside the mode coupling region. The observations were carried out from 7^h52^m until 10^h34^m UT with an 8-min interval between the scans.

We believe that the region of the B effect reflects the processes that take place in the region of coupling between the ordinary and extraordinary modes, because polarization inversions in frequency and time are commonly observed here (see also Fig. 6).

Multiple Spectral and Temporal Circular Polarization Reversals in FPARs

Our study of several FPARs indicates that a polarization inversion is often present in their microwave radiation and is probably a characteristic property of

ARs and should be investigated further. A polarization inversion commonly appears in the polarization spectrum before an intense flare and can also occur during the flare itself. Figure 6 shows the observations of AR 9393 carried out on April 5 at 9^h08^m UT immediately before the onset of the main phase of an M8.4 limb flare at 9^h22^m UT. We see four polarization inversions in frequency marked by the arrows on the right.

Our multi-azimuthal observations also revealed fast temporal variations of the polarization pattern in the wavelength range from 2 to 8 cm with an 8-min interval between the scans for 4 h. Figure 7 shows the observations of the FPAR 9415 on April 14, 2001, at 9^h54^m UT in the intensity and polarization channels at 13 wavelengths. We see that the degree of polarization decreased sharply in the wavelength range 2.67–3.21 cm. Therefore, this range is shown in Fig. 7c on a large scale. Interestingly, pointlike polarized radio sources with sharp variations over the spectrum up to the sign reversal appear in this range.

To analyze the temporal variations in the parameters of FPAR 9415, we selected two wavelengths shown in Fig. 8. One ($\lambda_1 = 2.90$ cm) was taken from the mode coupling region and the other ($\lambda_2 = 3.83$ cm) was taken from the long-wavelength range outside it. The figure shows 22 scans for the two wavelengths with a 8-min interval. For comparison with other ARs, we drew the vertical lines. The structure of AR 9415 at $\lambda_1 = 2.90$ cm consists of various narrow polarized radio sources with frequent polarization inversions in time. On the other hand, only smooth variations in the amplitude of the polarized signal occur at $\lambda_2 = 3.83$ cm.

THE RESULTS OF A STATISTICAL ANALYSIS

We performed a statistical analysis of the correlation of FPARs with detected features in the microwave radiation and with the productivity of intense flares. For our analysis, we chose the period from January through October 2001. In this year, three observations were carried out daily with RATAN-600 at various azimuths. The flaring activity in the period being analyzed is presented in Table 1. The table lists all of the FPARs that produced the most intense flares. Columns 3 and 4 characterize the X-ray activity; columns 5 and 6 characterize the optical activity.

The intense FPARs listed in Table 1 exhibited the features in the polarization spectrum described above. We experimentally established that all of the ARs that produced at least three intense flares of importance M or higher could be placed into this group. Only two regions, AR 9488 and AR 9636, which produced only

two intense flares each, constitutes an exception. Another exception is AR 9658, which produced 16 X-ray flares, four of which are of importance M, but we found no features in the spectrum of its circular polarization.

The results of our statistical analysis are presented in Table 2. We see from this table that almost all of the activity from January 4, 2001, through October 28, 2001, was attributable to the activity of the FPARs that accounted for only 5.9% of the total number of ARs regions on the Sun. The FPARs produced 83.3% of the intense flares, which usually generate high-velocity protons. Only one region of the 24 FPARs exhibited no features in the polarization spectrum. Such a high correlation coefficient may indicate a high prognostic value of the detected effects.

DISCUSSION

This paper emphasizes the importance of radio observations in studying the nature of the powerful flaring activity, because they are highly sensitive to polarization measurement, which is the main subject of discussion.

ARs should be distinguished by the stability of their radiation: stable, quasi-stable, and FPARs. All three types of ARs differ by the height distribution of plasma parameters.

Stable ARs produce no flares at all and they account for most of the ARs. These ARs have stable magnetospheres and the magnetic-field structure can be calculated in the potential approximation from the photospheric level into the corona. There is no substantial energy release in these ARs and the following condition is dominant: $E \leq H^2/8\pi$, where $E = n_e k T_e$ is the kinetic electron energy and H is the magnetic field.

Quasi-stable ARs produce several low- and medium-intensity flares (of X-ray importance A, B, or C) and, occasionally, one or two M flares. In general, they retain stable magnetospheres, but conditions with short-duration energy release in the form of intermediate-level flares can be created in them.

FPARs usually generate at least three intense flares of importance M or higher and many A, B, and C flares. FPARs are fundamentally unstable ARs. Energy is continuously released and accumulated in these regions and the condition $E \leq H^2/8\pi$ is satisfied here. The magnetospheres of these ARs are unstable, have no ordered structure, and cannot be calculated as an extrapolation of the potential magnetic field from the photosphere into the corona. This view explains the short (20–30 min) preflare phase in quasi-stable ARs (Kundu *et al.* 2001) and the long (from several hours to several days) preliminary phase in FPARs. The abrupt polarization inversions

Table 1. A list of FPARs from January through October 2001

NOAA AR number	Number of M and X X-ray flares	Total number of X-ray flares	Number of optical S-level flares	Number of optical flares with level >S
9313	4M	10	15	4
9368	3M	10	11	4
9373	4M	19	36	1
9393	24M, 3X	55	12	3
9401	5M	12	29	5
9415	6M, 5X	26	34	9
9433	15M	60	83	4
9455	5M	25	28	5
9488	2M	13	18	5
9502	3M	6	7	3
9511	4M, 1X	18	24	5
9557	3M	26	36	2
9591	9M, 1X	59	80	8
9600	3M	11	8	4
9601	10M	33	56	9
9608	12M	38	37	10
9616	5M	14	23	6
9628	7M	31	81	5
9632	2M, 1X	12	34	1
9636	2M	11	36	2
9658	4M	16	30	3
9661	1M, 2X	19	37	5
9672	4M, 2X	22	28	5
9682	9M	40	61	1

Table 2. The results of our statistical analysis for the period from January through October 2001

Number of all solar ARs from January 4, 2001, through October 28, 2001	406	100%
Number of FPARs that produced three or more M and X X-ray flares	24	5.9%
Number of all intense M and X X-ray flares	192	100%
Number of intense flares from FPARs	160	83.3%
Number of intense flares from FPARs with effects in microwave polarization spectra	156	81.2%

(see Figs. 7 and 8) over a long period suggest a continuously lasting flare process with weak energy release. This process accumulates energy in the AR magnetosphere and, subsequently, the mechanism of energy release is triggered.

Our observational data provide a new insight into the phenomenon of intense solar flares as the processes with a long preliminary phase. At this phase, weak energy release and accumulation in the AR magnetosphere take place. This process continues

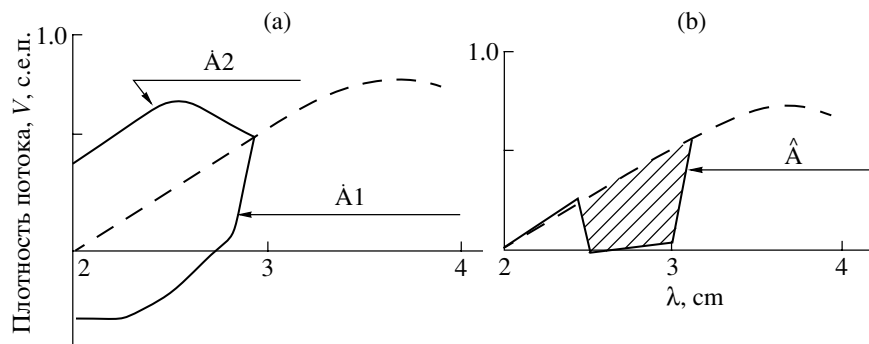


Fig. 9. (a) Comparison of the spectrum for a stable AR with a dominant cyclotron radio source and the spectrum for a FPAR with the A1 and A2 effects. (b) The same in comparison with the B effect.

until the instability level is reached. The subsequent scenario for the main flare phase was well developed (Petchek 1964; Heyvaerts *et al.* 1977; Shibata 1998; Zaitsev and Stepanov 1983). According to the RATAN-600 data in the wavelength range 2–5 cm, the preliminary phase can have several varieties in the polarization spectra of FPARs.

We treat two of them as the appearance of a new magnetic flux in the structure of the old overlying AR magnetic field. The polarity of the new magnetic flux can be identical to the dominant magnetic field polarity and, in this case, the polarization spectra exhibit a brightening toward shorter wavelengths (Fig. 4b). When a new magnetic flux with the polarity opposite to that of the old magnetic field rises, a short-wavelength polarization inversion is observed (Fig. 2b). These two effects persist in FPARs for several hours and days and, thus, differ from the so-called preflare phase. The latter generally lasts several minutes or, rarely, several tens of minutes (Kundu *et al.* 2001). The magnetic loops of the new magnetic flux appear to interact with the loops of the old magnetic field through reconnection according to the scenario of Hanaoka (1996). However, here, this process acts as a preheating. As a result, energy is accumulated in the AR magnetosphere to a level at which the magnetic structure becomes unstable, which triggers intense energy release and coronal mass ejection (see the review of Shibata 1998).

Another manifestation of the long preliminary phase found in radio observations is the formation of a frequency-limited region of coupling between the ordinary and extraordinary modes. Abrupt variations in the polarization pattern in the frequency band 20–25%, in which the degree of polarization decreases to fractions of a percent and in which the formation of pointlike polarized radio sources with sign reversals is observed (see Figs. 5a, 5b, 7, 9a), justify this name. Here, we probably also deal with weak energy release in higher layers of the lower corona. The multiple polarization inversions, both in frequency and in time,

indicate that the preliminary phase can arise in the form of long-duration low-energy miniflares. Such long-duration miniflares also result in the accumulation of energy in the magnetosphere, the attainment of the instability threshold, and the turnon of the main phase of an intense flare.

Based on the data obtained during 2001, we constructed generic spectra for the A and B effects (see Fig. 9).

What are the mechanisms of the detected spectral-polarization properties of the microwave radio emission (B effect) at the preliminary phase of intense flares? The discussion of this question is beyond the scope of this paper. Here, we only list basic properties of this effect:

(1) The frequency inversions occur in the wavelength range 2–5 cm, suggesting a connection to the magnetobremstrahlung mechanism at the first three or four gyrofrequency harmonics.

(2) The polarized flux in the mode coupling region decreases sharply to 0.05–10 s.f.u and the degree of circular polarization falls to 0.3–1%. Explanations of the presence of current sheets in the FPAR magnetosphere should probably be invoked.

(3) The polarization inversions at the preliminary flare phase occur at intervals of 8 min or, possibly, shorter.

(4) Multiple polarization inversions in frequency occur, suggesting a strong vertical magnetic field nonuniformity at the preliminary phase and during flares.

Magnetic reconnection is the most plausible interpretation. On the other hand, we cannot rule out the possibility that the frequency region results from the turbulence of a multiarch magnetic structure or many current sheets on the pathway of radio waves to the Earth (Zheleznyakov *et al.* 1996). The model of Zlotnik (2001), which explains the polarization inversion as resulting from the appearance of an ordinary mode in the cold plasma of a prominence located above a

hot radio source, should also be mentioned. However, this model disregards the turbulence of cold and hot plasmas.

CONCLUSIONS

(1) Based on the RATAN-600 spectral-polarization observations, we obtained a new observational result concerning the properties of the magnetospheres of FPARs in their polarized radiation.

(2) We obtained data on the existence of a long preliminary phase during the generation of intense flares, which manifests itself in detailed polarization spectra over a wide microwave range.

(3) We introduced the concept of FPAR with long-duration energy release at the preliminary phase, energy accumulation, and explosive energy release during the main phase.

(4) We provided statistical data that shows a special role of FPARs in the general solar activity.

(5) We showed the necessity of using large instruments in investigating FPARs both when studying the physical processes and when developing prediction criteria for intense flares.

Because of their high sensitivity to the processes in the lower corona, where primary energy release takes place, spectral-polarization radio observations can form the basis for developing techniques for predicting intense flare events, which are often accompanied by the release of a large number of high-energy protons.

Thus, spectral radio observations are important in understanding the physical processes in FPARs and for applied problems, for example, those associated with the Cosmic Weather Program.

ACKNOWLEDGMENTS

We wish to thank the staff of RATAN-600 for help with the observations and V.I. Makarova for a fruitful discussion. This study was supported in part by the Russian Foundation for Basic Research (project no. 02-02-16430) and the INTAS-00-181.

REFERENCES

1. Sh. B. Akhmedov, G. B. Gelfreikh, V. M. Bogod, and A. N. Korzhavin, *Sol. Phys.* **79**, 41 (1982).
2. V. M. Bogod, A. Grebinskij, V. Garaimov, *et al.*, *Bull. Spec. Astrophys. Obs.* **47**, 5 (1999).
3. V. M. Bogod, V. I. Garaimov, N. P. Komar, and A. N. Korzhavin, *ESA Spec. Publ.* **448**, 1253 (1999).
4. V. M. Bogod, S. M. Vatrushin, V. E. Abramov-Maximov, *et al.*, *Astron. Soc. Pac. Conf. Ser.* **46**, 306 (1993).
5. M. H. Cohen, *Astrophys. J.* **131**, 664 (1960).
6. A. E. Covington, *Sol. Phys.* **33**, 439 (1973).
7. V. I. Garaimov, *Preprint Spec. Astrophys. Obs. Ros. Akad. Sci.* **27**, 1 (1997).
8. D. E. Gary, M. D. Hartl, and T. Shimuzu, *Astrophys. J.* **477**, 958 (1997).
9. G. B. Gelfreikh, in *Solar Coronal Structures. Proceedings of the 144th Colloquium of the IAU, Tatranska Lomnica, Slovakia, 1993*, Ed. by V. Rusin, P. Heinzel, and J.-C. Vial (VEDA Publishing House of the Slovak Academy of Sciences, Tatranska Lomnica, 1994), p. 21.
10. Y. Hanaoka, *Sol. Phys.* **165**, 275 (1996).
11. J. Heyvaerts, J. M. Priest, and D. M. Rust, *Astrophys. J.*, **216**, 123 (1977).
12. G. J. Hurford, R. B. Read, and H. Zirin, *Sol. Phys.* **94**, 413 (1984).
13. M. M. Kobrin, A. I. Korshunov, S. I. Arbutov, *et al.*, *Sol. Phys.* **56**, 359 (1978).
14. D. V. Korol'kov and Yu. N. Parijskij, *Sky Telesc.* **57**, 324 (1979).
15. M. R. Kundu, V. Gaizauskas, B. E. Woodgate, *et al.*, *Astrophys. J. Suppl. Ser.* **57**, 621 (1985).
16. M. R. Kundu, V. V. Grechnev, V. I. Garaimov, and S. M. White, *Astrophys. J.* **563**, 389 (2001).
17. M. R. Kundu, S. M. White, K. Shibasaki, and J. P. Raulin, *Astrophys. J. Suppl. Ser.* **133**, 467 (2001).
18. K. R. Lang, R. F. Willson, J. N. Kile, *et al.*, *Astrophys. J.* **419**, 319 (1993).
19. V. P. Maksimov, V. P. Nefed'ev, and G. Ya. Smol'kov, *Issled. Geomagn. Aeronom. Fiz. Soln.* **82**, 155 (1988).
20. D. B. Melrose, in *Proc. of Nobeyama Symposium, Kiyosato, Japan, 1998* Ed. by T. S. Bastian, N. Gopalswamy and K. Shibasaki, *NRO Report* **479**, 371 (1998).
21. A. Nindos, M. R. Kundu, S. M. White, *et al.*, *Astrophys. J. Suppl. Ser.* **130**, 485 (2000).
22. H. E. Petcheck, in *Proc. AAS-NASA Symp. on Physics of Solar Flares, NASA SP-50* Ed. by W. N. Hess, (Washington, D. C., 1964), p. 425.
23. L. A. Pustil'nik, *Astron. Zh.* **50**, 1211 (1973) [*Sov. Astron.* **17**, 763 (1973)].
24. B. I. Ryabov, N. A. Pilyeva, C. E. Alissandrakis, *et al.*, *Sol. Phys.* **185**, 157 (1999).
25. K. Shibata, in *Proc. of Nobeyama Symposium, Kiyosato, Japan, 1998* Ed. by T. S. Bastian, N. Gopalswamy and K. Shibasaki, *NRO Report* **479**, 381 (1998).
26. H. Tanaka and S. Enome, *Sol. Phys.* **40**, 123 (1975).
27. V. V. Zaitsev and A. V. Stepanov, *Sol. Phys.* **88**, 297 (1983).
28. V. V. Zheleznyakov, *Radio Emission from the Sun and Planets* (Nauka, Moscow, 1964).
29. V. V. Zheleznyakov, V. V. Kocharovskiy, and V. V. Kocharovskiy, *Astron. Astrophys.* **308**, 685 (1996).
30. E. Ya. Zlotnik, *Radiophys. Quantum Electron.* **44**, 53 (2001).

Translated by V. Astakhov